Eng. Sci., 2022, **18**, 193–203

Engineered Science
DOI: https://dx.doi.org/10.30919/es8d677

Modelling of Interior Permanent Magnet Motor and Optimization of its Torque Ripple and Cogging Torque Based on Design of Experiments and Artificial Neural Networks

Ganesh C. J.,[1] Vijay G. S.[1] and Siddappa I. Bekinal[1,*]

Abstract

Interior permanent magnet (IPM) motors are a class of synchronous motors. They are known for their high-power density and effective speed control performance along with efficient torque per rotor volume. They are also capable of giving wide constant power operating range which makes them best suitable for electric vehicle applications (EV sector). However, the major task in the design of any IPM motor is the optimization of torque ripple and reducing the undesirable cogging torques. Rotor geometry is the primary design criterion in reducing torque pulsations. In this work, the orthogonal experimental design (OED) is used for optimizing rotor geometry to discover the ideal combination of geometric parameters to reduce torque pulsations and cogging torques. An artificial neural network (ANN) is then modeled to find the optimum design for rotor geometry using metaheuristic algorithms. Finally, the results of the optimization process are verified by the conventional finite element analysis (FEA) method. Torque ripple and cogging torque are reduced by 65% and 12% respectively on post-optimization.

Keywords: IPM Motor; cogging torque; Torque ripple; Design of Experiments; Artificial Neural Networks.
Received: 23 October 2021; Revised: 09 March 2022; Accepted: 12 March 2022.
Article type: Research article.

1. Introduction

An electric motor is a machine that converts electrical energy into mechanical energy by rotation of the shaft giving a torque output. This happens due to the interaction between the magnetic field present in the rotor and the current flowing through the winding. The major problem encountered is the generation of torque pulsation resulting in vibration of the motor, which is optimized to a certain level that will yield a low noise of the motor during its operation.[1] Electric machines that produce magnetic fields by permanent magnets are called permanent magnet (PM) machines. The high-power density and speed control properties of interior permanent magnet synchronous motors (IPMSM) are well-known. Minimizing the torque ripple or pulsation is always one of the major trends in the design of IPMSM.[2] When IPMSM is rotated there exists always a certain level of torque ripple or pulsation which is one of the major drawbacks of operating an interior permanent magnet (IPM) machine, resulting in the noise and vibration of the motor. There are various methods of optimizing such torque pulsation and undesirable cogging torques. Electric parameters can be varied to optimize the torque pulsation by varying the winding distributions.[3] Another reason for torque pulsation is due to variation in the reluctance of the magnetic circuit during the full rotation of the rotor which can be influenced by magnetization direction, the number of slots, winding distribution, and skew angle.[4]

The major reason for undesirable torque ripple could be the non-ideal magnetic field distribution which may be due to the poor design of the electric motor. This will also result in the cogging torque which will ultimately reduce the desired torque output of the motor. Another method of optimizing the torque pulsation and the undesirable cogging torques is the geometry of the rotor of the IPM. Optimization of rotor geometry is one of the vital design criteria of electric machines. Several such design parameters were analyzed by various researchers. Zhu *et al*. adjusted the geometry of the motors employing the response surface technique and the Taguchi method after studying the design variables of IPMSM based on the relevance of the parameters to be optimized.[5] They were able to optimize the torque ripples, keeping the motor output torque constant. Kioumarsi *et al.* proposed a method of drilling minor

[1]*Department of Mechanical and Industrial Engineering, Manipal Institute of Technology, Manipal Academy of Higher Education, Manipal -576104, Udupi, Karnataka, India.*
**E-mail:* siddappa.bekinal@manipal.edu (S. I. Bekinal)

holes in the rotor to minimize the torque pulsation in IPM.[6]

The influence of the rotor pole on the pole pitch ratio of the cogging torque of an IPM machine was presented by Zhu *et al*.[7] Hwang *et al*. proposed the design and electromechanical properties of IPM motors as a function of rotor shape.[8] They considered speed, torque, torque ripple, and back electromotive force (B-EMF) voltage as various factors for their comparison. Ma *et al*. study focused on flux weakening techniques and reducing the vibrations of IPM motors.[9] They optimized cogging torque and torque ripples successfully.

Torque control and design optimization of the motor using advanced computer simulation to enhance the performance and efficiency of the electric motor is the latest trend. Zhang *et al*. offered a study focusing on the optimization of cogging torques and torque ripple, which cause vibrations and electromagnetic flux variations.[10] They attempted to optimize the dimensions of the rotor's essential geometries. Configuring the design of the rotor involves the positioning of the magnets, types of permanent magnet materials, robustness, and simplicity of construction to get optimum output. The rotor arrangement of an IPM motor is a critical aspect in determining the motor's overall performance. Zhu *et al*. investigated and compared the electromagnetic behavior of multilayered IPM devices for EV applications.[11] The three-layered IPM machine has reduced torque ripple and core loss because the harmonics of air-gap density are lowered as the number of magnet layers increases.

A finite element analysis (FEA) method was utilized by Hwang *et al.* to investigate the properties of IPMSM that are employed as drive motors in electric cars in their study.[12] The stator and rotor's external diameters were adjusted to be the same so that various parameters including cogging torque, torque ripple, and back emf voltage could be compared depending on the position of a notch on the rotor shape. In their study, Hwang *et al*.[13] developed an effective method of optimizing the rotor design in such a way that the flux distribution in the core is changed.

K. I. Laskaris and A. G. Kladas presented an improved IPM motor with high torque and exceptionally high efficiency in the same working area.[14] When compared to a surface permanent magnet (SPM) motor of the same size, the proposed technique has the advantage of magnetic flux concentration in the air gap, allowing for significantly higher magnetic flux density values. Zheng *et al*. suggested an IPM machine with numerous rotor topologies, and the various IPM machines were assessed, notably for drive applications.[15] All IPM machines were discovered to have been tuned to generate high torques while decreasing pulsation and cogging torques. Because of the extremely nonlinear magnetic behavior, conducting an exact analytical computation to predict motor performance is quite difficult. In the design of any IPM machine, conventional numerical methods, including FEA, are frequently employed. In optimizing the design of a rotor or any component, one of the most commonly used methods in industries is one factor at a time (OFAT), in which most design factors are maintained constant, and one factor is modified until the desired output is reached. This approach is time-consuming and inefficient at times owing to its inability to consider more than one variable at the same time.

Another effective method of optimizing the design variables is the design of experiments (DOE) where we can study the behavior of multiple factors changing simultaneously and also the interactions between these variables. However, when optimization of IPMSM with one or more of the design factors to minimize torque ripple, the motor architecture becomes more complicated, and the structural parameters linked to motor output performance become higher, making IPMSM topology optimization very challenging. When there are many structural features to be changed, the response surface approach becomes extremely difficult.[16]

One of the challenges in PM electric machine design is reducing cogging torque. To improve the performance of brushless direct current motors using the DOE technique, a novel method for designing motor magnets is provided. The DOE approach is used to screen the design space and generate approximation models with response surface techniques.[17] When there are numerous structural variables to be improved, an optimization technique that combines an algorithm with FEA software takes a long time.[18,19] The Taguchi approach can execute multi-objective optimization on an IPMSM; however, it is unable to find the optimum parameter combination, resulting in a poor optimization result.

In motor design, the selection of suitable design parameters to match the specified operating requirements is essential. As a result, regression analysis stated in terms of design variables is necessary for design optimization. The purpose of regression analysis is to determine how an objective function changes in response to changes in design factors. The use of such regression analysis in conjunction with optimization techniques yields the best design parameters.

Because ANN training requires a significant quantity of data and gathering data takes a long time when the number of structural variables to be optimized is enormous.[20] In recent years, the IPM machine rotor was optimized based on genetic algorithms (GA).[21] The nonlinear characteristics of diverse systems can be estimated using an ANN. It has been used in several research projects to aid in the design of various electric machines. The size of the induction motor, as well as the cost of manufacture, are optimized using ANN-based design.[22] It is also used to design an induction motor based on FEA results to optimize the rotor slot geometry to maximize the average torque.[23] To reduce the torque ripple of an IPMSM, Hao *et al*. performed range analysis on the data obtained from the orthogonal experiments to calculate the optimum combination of geometric parameters using multi-island genetic algorithm (MIGA) and radial basis function (RBF) neural networks.[24]

The main objective of this article is to overcome undesirable cogging torque and torque ripple by a systematic design of geometry for IPM machines using DOE and ANN. It's been observed that while trying to reduce the cogging

torque, the torque ripple tends to increase and vice versa resulting in conflicting behavior. Training an ANN model requires collecting numerous existing and established sets of simulation data. But to make the optimization process more flexible and adaptable for machines with various sizes and requirements, this study employs an effective way of extracting regression equation from orthogonal experimental design and later using it with metaheuristic algorithms such as multi-objective particle swarm optimization (MOPSO) and JAYA algorithm to reduce cogging torque and torque ripple simultaneously.[25-28]

2. Methodology

2.1 Optimization process

The proposed optimization process to lower the motor torque ripple and cogging torque is presented in the form of a flow chart as shown in Fig. S1. The steps followed in the optimization process are given below:

1. The objectives of the optimization were defined at first;
2. The geometric parameters to be optimized were selected based on the objectives;
3. An orthogonal array for the design of experiments was defined based on the number of design variables and their levels;
4. The orthogonal experiment-based simulations were conducted using Ansys Motor-CAD software;
5. A multi-objective-based regression equation was extracted;
6. Discrete data from the DOE was then converted into continuous form by applying ANN methods;
7. Metaheuristic algorithms were developed and used to carry out the optimization to identify the optimal values of the design variables;
8. The result of the above process was then verified using conventional methods.

2.2 Initial IPM model

A 3-phase, 10-pole, 12-slot IPM motor as shown in Fig. 1 was modeled for this study. The geometric design parameters which were to be optimized per the objective are shown in Table 1. To design and optimize the rotor dimensions and to perform simulations, Ansys Motor-CAD software was used. The initial design of the IPM was limited to a 1 kW application with an average peak power of 1.1 kW and the parameters selected are given in Table 2.

Table 1. Motor Design Variables.

Design Variable	Abbreviation	Value	Unit
Magnet thickness	t	4	mm
Magnets embed depth	d	2.5	mm
Magnet arc (ED)	α	140	Degree
Air gap	Ag	0.7	mm

Several parameters such as magnet thickness, depth from rotor periphery, air gap, and magnet arc can be taken as inputs for evaluating the outputs such as cogging torque, and torque ripple as per Eq. (1).

$$y = f\,(t, d, \alpha, Ag) \quad (1)$$

Each of these design variables is defined within certain limits: lower limit ≤ x ≤ upper limit.

Table 2. Parameters of IPM.

Design Variable	Value	Unit
Poles	10	
Slots	12	
Stator lam diameter	130	mm
Stator bore diameter	80	mm
Magnet length	40	mm
Magnet Br	1.31	Tesla
Rated shaft speed	2000	RPM

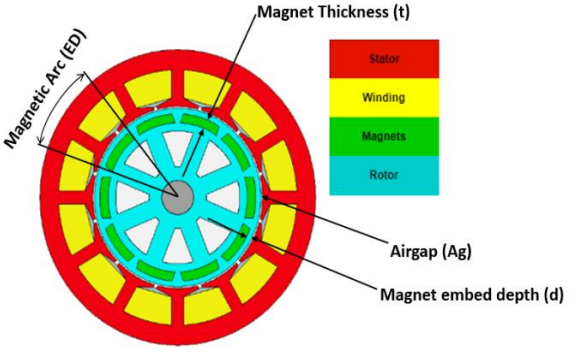

Fig. 1 Cross-section of IPM.

The limits for the design variables are considered based on the prior calculations and boundary limits of the design of the motor and other mechanical constraints to avoid any possible conflicts. The objective functions are set to minimize the cogging torque and torque ripple.

3. Optimization of cogging torque and torque ripple

3.1 Orthogonal experimental design

Orthogonal experimental design is one of the widely used methods to determine the optimal values for the variables. Experiments here are referred to the computer-based motor CAD simulations. While evaluating the effects of various design variables or parameters on any system response, a systematic method must be adopted which involves a series of simulations to cover all possible domains of the design considered.

The traditional design process is ineffective for a variety of reasons, including the fact that the number of experiments to be run will be too vast to implement with the number of design parameters available. Instead of performing prototype simulations or a thorough experimental design, which is time-consuming and inefficient, the OED approach can be utilized as an effective way for conducting computer simulations, providing adequate system knowledge for further usage.

The reduction in the number of experiments is one of the most notable benefits of using the OED optimization approach. The OED approach makes use of a matrix called an orthogonal array (OA). The parameter values in each combination are

represented by each row of the matrix, and the number of rows indicates the predicted number of experiments in each design. The orthogonal array's columns represent a parameter, and the number of columns equals the number of design parameters. Once the design variables are finalized, OED can be set up and design experiments can be evaluated by following the steps given below:

1. Consider only the critical design variables;
2. Decide the number of values\levels each variable must carry;
3. Generate the orthogonal array for the considered design variables and their levels based on the principles of DOE;
4. Perform simulations for each set of experiments of OA to extract their respective responses;
5. The system is then modeled using ANN methodologies with the aid of regression analysis to obtain optimal design by applying metaheuristic algorithms.

Four critical rotor design variables are defined to apply orthogonal array DOE for the IPM machine under consideration. The present experimental design aims to find the optimal values for the rotor geometry for which the IPM motor has minimum cogging torque and torque ripple. The cogging torque and the torque ripple are made as to the system output response. The values for 4 different rotor geometries are tabulated in Table 3. Now by considering 5 levels for each parameter an L25 (5^4) orthogonal array (Table S1) had been designed and Motor-CAD simulations were carried out.

L: Orthogonal Array *25: Number of experiments*
5: Number of values *4: Number of Parameters*

Table 3. Values for Design Parameters of IPM.

Design Parameter	Levels of Design Parameter				
t	3	3.5	4	4.5	5
d	1.5	2	2.5	3	3.5
α	130	135	140	145	150
Ag	0.5	0.6	0.7	0.8	0.9

By employing the OED method, the number of experiments is reduced from massive $5^4 = 625$ to 25 experiments. Even though conventional full experimental design provides sufficient information, it may require too much effort to set up and is time-consuming. The suggested OED technique will greatly cut computation time and design effort without sacrificing critical information. If the complete experimental design approach is utilized in the given PM machine example, the OED method requires less than 5% of the overall computation time. This will result in the efficient use of resources to properly design the system within a stipulated time.

3.2 Regression model

Regression analysis is a predictive modeling approach that examines the connection between a dependent (target) variable(s) and an independent variable(s) (predictor). This technique uses forecasting, time series modeling, and identifying the causal impact connection between variables. In this work, a significant effect of each input variable on cogging torque and torque pulsation is studied. Simulation results of an orthogonal array are given in Table S2. It has been observed that each of the 25 experiments has given different responses. Fitting a regression model helps to analyze the significance of each of the input factors. The link between two or more variables was estimated using regression analysis. The degree of the impact of numerous independent factors on a dependent variable can also be determined using regression analysis. It can be seen from the simulated results that each of the different experiments is giving different outputs for cogging torque and torque ripple. It is also observed that optimizing the cogging torque is leading to the rise of torque ripple and vice versa. To solve such a condition, we are adopting a multi-objective optimization method.

Regression fit and ANOVA (Analysis of Variance) was performed on the set of simulation data using Minitab software. The regression equations for the fitted responses torque ripple and cogging torque are as per Eq. (2) and Eq. (3) respectively.

$$Torque\ ripple = -10.04 + 0.153t + 0.333d + 0.1421\alpha - 1.22Ag - 0.0089t^2 + 0.238d^2 - 0.000542\alpha^2 + 0.773Ag^2 - 0.0966t*d + 0.00258t*\alpha - 0.7791t*Ag - 0.0149d*Ag \quad (2)$$

$$Cogging\ torque = 1.02 - 0.547t - 0.1994d + 0.0235\alpha - 3.392Ag - 0.02439t^2 + 0.0182d^2 - 0.000163\alpha^2 + 0.954Ag^2 - 0.0922t*d + 0.00684t*\alpha + 0.0965t*Ag + 0.4465d*Ag \quad (3)$$

Residual plots for the fitted regression equations are shown in Fig. 2. The main effects plots of all four factors on the responses are shown in Fig. 3. The results of effect plots show that torque ripple increases steadily with the thickness of the magnet. Cogging torque is minimal at a certain optimal value for magnet thickness and beyond which it tends to increase. Both torque ripple and cogging torque tend to decrease with an increase in the air gap. Torque ripple will increase with the increase in the magnetic arc angle and then decrease after a certain point. Cogging torque will decrease with an increase in the magnetic arc angle and then increase after a certain point. Torque ripple increases with an increase in the depth of magnet placement, whereas the cogging torque decreases with the increase in depth of magnet placement. Conflicting behavior is observed between the geometrical parameters over the two measured responses.

Now on performing multi-response optimization to minimize torque ripple and cogging torque simultaneously. Limits are defined for performing multi-objective response optimization. The goal is to minimize the torque ripple and cogging torque. The predicted responses by DOE using Minitab software are shown in Table 4 and the respective experimental simulation results for the optimized set of values are shown in Table 5. The shaft output torque for the above DOE optimized setting was found to be 3.69 Nm with torque ripple accounting for around 3.75%.

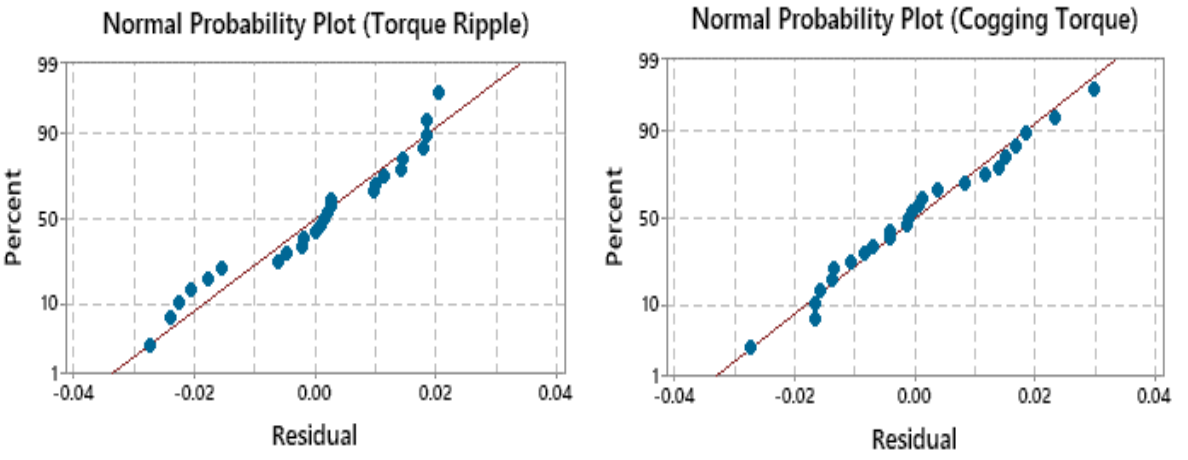

(a) (b)

Fig. 2 Residual plots (a) Torque ripple (b) Cogging torque.

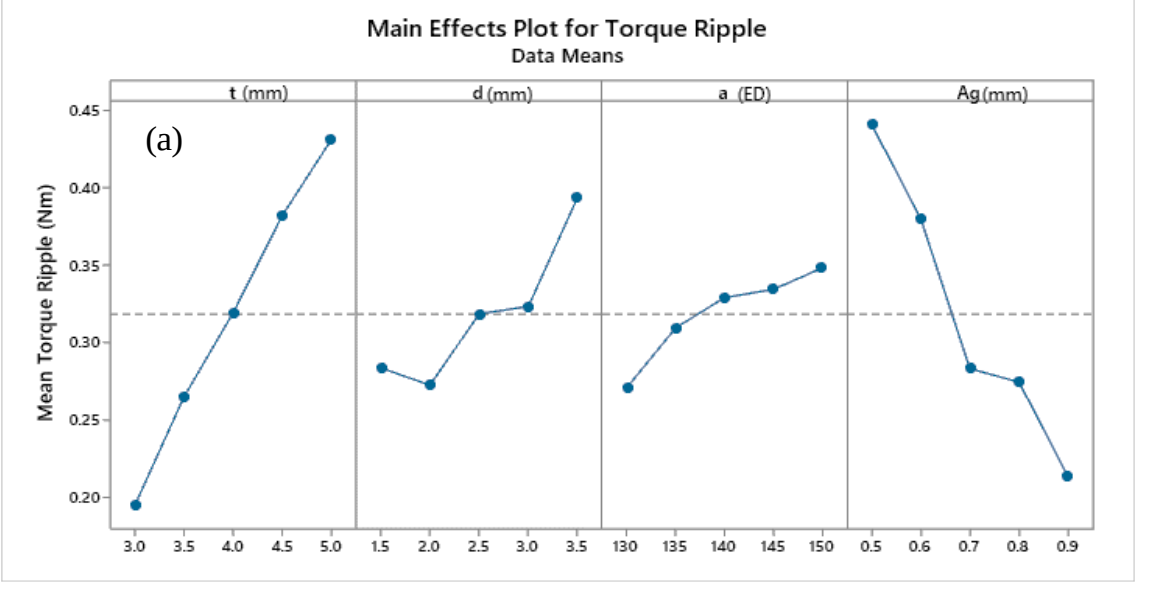

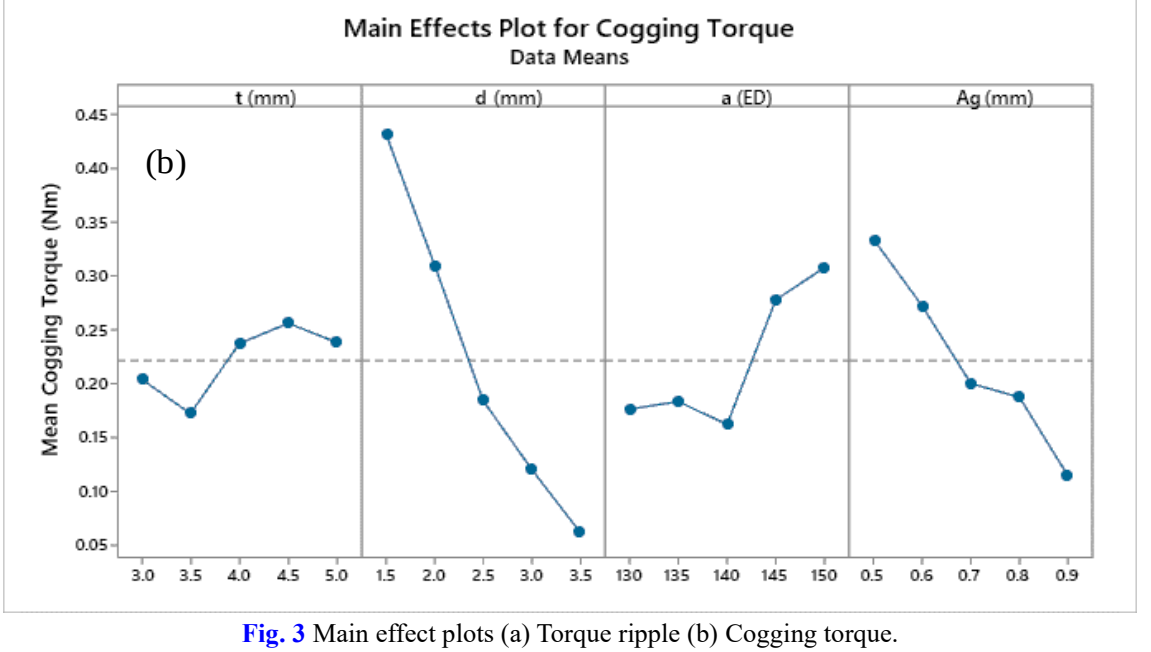

Fig. 3 Main effect plots (a) Torque ripple (b) Cogging torque.

Table 4. Multiple response prediction.

Design Variable	Abbreviation	Value	Unit
Magnet thickness	t	3.505	mm
Magnets embed depth	d	1.5	mm
Magnet arc (ED)	α	141.11	degree
Air gap	Ag	0.9	mm

Table 5. Experimental simulation results for DOE optimized set of values.

Design Variable	Value	Unit
Torque Ripple	0.13	Nm
Cogging Torque	0.17	Nm

3.3 The artificial neural network model

The single hidden layered feed-forward ANN as shown in Fig. S2 was used to fit a predictive model between the four inputs (x_1 = t, x_2 = d, x_3 = α and x_4 = Ag) and the three outputs (O_1 = Torque ripple, O_2 = Cogging torque and O_3 = Shaft output torque). w_{ji} is the weight on the arrow connecting the j^{th} hidden neuron to the i^{th} input neuron, and β_{jk} is the weight on the arrow connecting the j^{th} hidden neuron to the k^{th} output neuron. b_{hj} and b_{Ok} represent the weights on the biases of the hidden neurons and the output neurons, respectively. The configuration of the ANN design was designated as 4: L : 3. The number of hidden neurons L was varied from 5 to 50. The termination criteria set are: the maximum number of epochs = 1000, minimum mean square error (MSE) = 1×10^{-8} and minimum gradient = 1×10^{-12}. The ANN would terminate if any one of these criteria were met. The configuration with the least MSE and least mean absolute percentage error (MAPE) was selected. The configuration with L = 11 was selected for the study as the corresponding MSE was 2.138×10^{-8} and MAPE was 4.21×10^{-4}. Only 92 epochs were sufficient to train the ANN. The training stopped on reaching the minimum gradient. Fig. S3 shows the MATLAB representation of the ANN configuration 4:11:3. The training curve for the same is shown in Fig. 4. The tan*sigmoid* activation function was applied on the hidden layer output whereas the *purelin* activation function was applied on the output layer computations. The ANN model gave a very good fit with an R^2 value of 0.9999, 0.9999, and 0.9999 for the three outputs O_1, O_2, and O_3, respectively. Table 6 compares the quality of fit given by the regression model and the ANN model in terms of the R^2 values. The ANN model gives a better fit and thus the ANN model is used to define the objective functions in the optimization algorithms. For the trained ANN model, the weight matrix [w] on the hidden layer, the weight matrix [β] on the output layer, the bias vector $\{b_h\}$ on the hidden layer, and the bias vector $\{b_O\}$ on the output layer are given Table S3.

Table 6. Quality of fit given by the Regression model and the ANN model.

	Torque ripple	Cogging torque
R^2 (Regression model)	0.9983	0.9975
R^2 (ANN model)	0.9999	0.9999

3.4 Optimization using metaheuristic algorithms: PSO and JAYA

Although computer simulations utilizing the OED technique offer enough information with considerably fewer data points, the optimal rotor design cannot be obtained based on the limited data points. This is because there are only a few sparse spots accessible over the whole design area, and there is a significant chance that the perfect point will be overlooked. Furthermore, there are just a few discrete FEA data points accessible. To find the global optimal rotor design, the values of each parameter must be swept continuously. A mathematical model must be created to anticipate torque pulsations and cogging torque for various rotor designs. Due to the highly non-linear behavior of the magnets used in the rotor, it becomes difficult to match and bring a mathematical relation.

As the ANN model provides a better quality of fit (evident from Table 6), this research employs the ANN model to assist the optimization process by executing complicated tasks that are hard to interpret using explicit mathematical equations. IPM motor optimization was performed based on the Regression model and ANN model generated from computer simulations with various rotor geometries. Three multi-objective optimization techniques were compared:

- OED-based optimization, using the desirability function approach by MINITAB software
- Particle Swarm Optimization (PSO), a swarm intelligence approach
- JAYA algorithm, an integrated evolutionary and swarm intelligence approach

The PSO technique is made up of a group of particles that move throughout the search space based on their own best previous location as well as the best past location of the entire swarm or a close neighbor. The velocity of a particle was adjusted in each cycle using Eq. (4),

$$V(t+1) = (t) + C1 * \text{rand}(R1) * (Pi\_best - (t)) + C2 * \text{rand}(R2) * (Pg\_best - Pi(t)) \quad (4)$$

where Vi (t + 1) is the updated velocity for the i^{th} particle. C1 and C2 are the personal best and global best weighting coefficients, respectively. Pi(t) is the location of the i^{th} particle at time t. R_1 and R_2 are random numbers in the range of 0 to 1. The most well-known position is Pi_best. Pg_best is the most well-known swarm position

This update equation's variants consider the optimal placements inside a particle's immediate neighborhood at time t. The location of a particle was updated using Eq. (5). A standard multi-objective particle swarm optimization

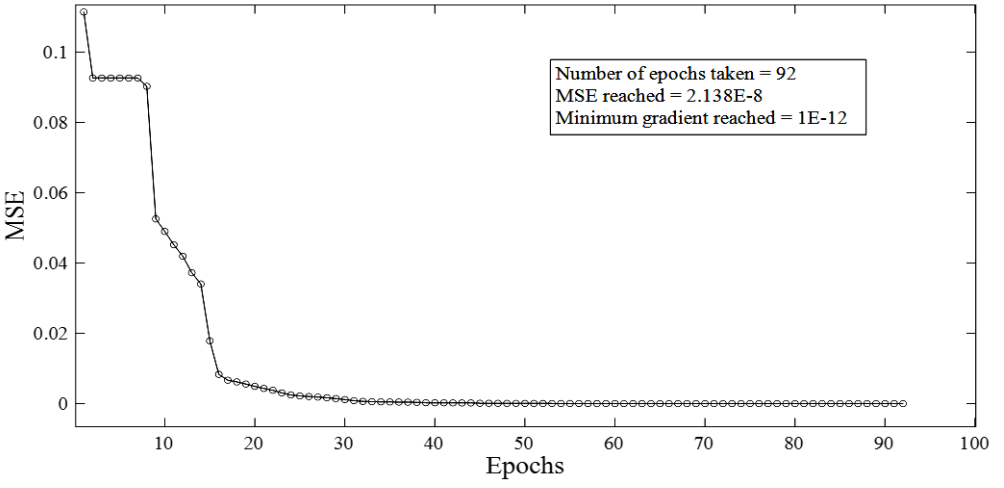

Fig. 4 The training curve for the ANN configuration 4: 11: 3.

(MOPSO) the algorithm was created using MATLAB. The optimal values of the essential geometric parameters (Table 7) were determined using MOPSO in this work. The objective function and constraints used in the optimization are given in Eq. (6).

$$P(t+1) = (t) + (t) \tag{5}$$

$$\left.\begin{array}{c} Minimize\ Cogging\ Torque \\ Minimize\ Torque\ Ripple \\ 3 \le t \le 5 \\ 1.5 \le d \le 3.5 \\ 130 \le \alpha \le 150 \\ 0.5 \le Ag \le 0.9 \end{array}\right\} \tag{6}$$

Table 8 displays the optimization outcomes. Post optimization by MOPSO, the torque ripple, and cogging torque were reduced significantly, while the output torque remained fundamentally unchanged at the desired range.

Table 7. MOPSO Prediction.

Design Variable	Abbreviation	Value	Unit
Magnet thickness	t	3	mm
Magnets embed depth	d	1.5	mm
Magnet arc (ED)	α	130	degree
Air gap	Ag	0.873	mm

Table 8. Experimental simulation results for MOPSO optimized set of values.

Design Variable	Value	Unit
Torque ripple	0.12	Nm
Cogging torque	0.15	Nm

The shaft output torque for the above MOPSO optimized setting was found to be 3.65 Nm with torque ripple accounting for around 3.6%.

The JAYA method integrates features of EA (Evolutionary Algorithms) concerning survivability for the fittest concept, along with SI (Swarm Intelligence), wherein the Swarm accompanies the leader throughout the quest for the optimal solution. Rao[26] proposed the JAYA algorithm in 2016, and it has piqued the curiosity of a wide range of research communities due to its amazing characteristics: It has simple concepts and is straightforward to use. In the initial search, there is no derivative information. It's a no-parameter algorithm. It's versatile, flexible, and well-rounded. As a consequence, the JAYA technique has been widely used for a broad variety of optimization issues in a variety of fields.

MATLAB was used to build a proper JAYA algorithm for multi-objective optimization. JAYA was employed in this study to determine the best values of the essential design variables. The objective function and constraints used in the optimization are given in Eq. (7).

$$\left.\begin{array}{c} Minimize\ Cogging\ Torque \\ Minimize\ Torque\ Ripple \\ 3 \le t \le 5 \\ 1.5 \le d \le 3.5 \\ 130 \le \alpha \le 150 \\ 0.5 \le Ag \le 0.9 \end{array}\right\} \tag{7}$$

The Pareto optimal front for the Poloni function obtained from the JAYA algorithm is shown in Fig. S4.

The proposed JAYA approach has been implemented to optimize design variables simultaneously. The spread of the Pareto-optimal set over the trade-off surface is seen in Fig. S4. This method retains the variety of non-dominated solutions over the Pareto-optimal front while solving the issue effectively. Table 9 shows one non-dominated solution that represents the best cost among the non-dominated solutions obtained. Experimental simulation results for MOPSO optimized set of values are shown in Table 10.

Table 9. JAYA Prediction.

Design Variable	Abbreviation	Value	Unit
Magnet thickness	t	3	mm
Magnets embed depth	d	1.5133	mm
Magnet arc (ED)	α	130	degree
Air gap	Ag	0.9	mm

Table 10. Experimental simulation results for MOPSO optimized set of values.

Design Variable	Value	Unit
Torque ripple	0.12	Nm
Cogging torque	0.14	Nm

The shaft output torque for the above JAYA optimized setting was found to be 3.6 Nm with torque ripple accounting for around 3.5%.

4. Verification of results

Motor-CAD software was used to carry out calculations on the post-optimization motor torque ripple and cogging torque to ensure the correctness of the optimization results. Fig. 5 depicts the magnetic field patterns of the motors. Except for the higher flux concentration at the bridge, the magnetic field distribution of the redesigned IPMSM remained essentially unchanged. The comparison of post-optimization results of DOE, MOPSO, and JAYA techniques is shown in Table 11.

To validate the optimization results, the newly predicted set of inputs was fed into Motor-CAD software, and responses were extracted and compared with the of predicted results of optimization. A maximum deviation of 7.69 % was observed between the results of Motor-CAD and optimization.

The results revealed that the motor torque ripples were reduced by 65% after the optimization when compared to the initial design. Also, the cogging torque was reduced by 12% after optimization as compared to the original design. Further to that, the simulation results revealed that after the optimization, motor output torque was appreciably improved from that of the original design.

It is observed from Fig. 6 that post-optimization the shaft output torque had been significantly increased along with reduced torque pulsations.

Also, the mechanical reliability of the optimized model was cross-verified to ensure a safe design post-optimization of rotor geometry. Rotor Material: M250-35A (Yield Strength = 455 MPa). Mechanical stress and distortions were calculated using FEM methods in Motor-CAD software. The von Mises stress was 1 MPa, which was substantially smaller than the yield strength, indicating that the rotor design was both safe and durable. As demonstrated in Fig. 7 for the MOPSO optimized model, the maximum rotor distortion was substantially low at 0.00006 mm.

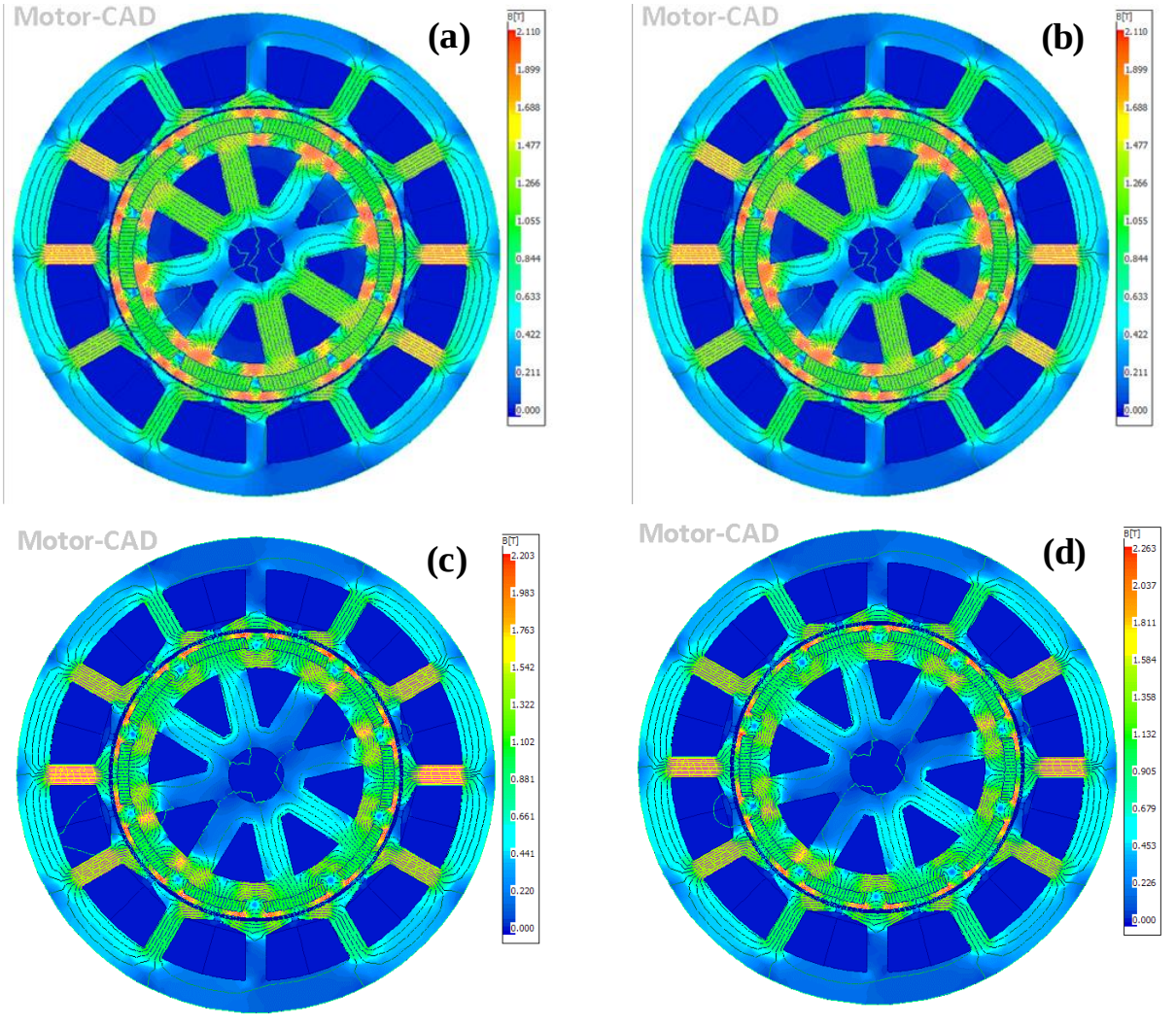

Fig. 5 Flux distribution for various optimized designs (a) original (b) DOE optimized (c) MOPSO optimized (d) JAYA optimized.

Table 11. Comparison of post-optimization results of DOE, MOPSO, and JAYA techniques.

		Predicted	Results of the Motor-CAD software	Variation in %
DOE	Torque Ripple (Nm)	0.13	0.14	7.69
	Cogging Torque (Nm)	0.17	0.178	4.71
	Output Torque (Nm)	3.69	3.693	0.08
MOPSO	Torque Ripple (Nm)	0.12	0.123	2.5
	Cogging Torque (Nm)	0.15	0.156	4.0
	Output Torque (Nm)	3.65	3.43	6.03
JAYA	Torque Ripple (Nm)	0.12	0.12	0.0
	Cogging Torque (Nm)	0.14	0.141	0.71
	Output Torque (Nm)	3.60	3.404	5.44

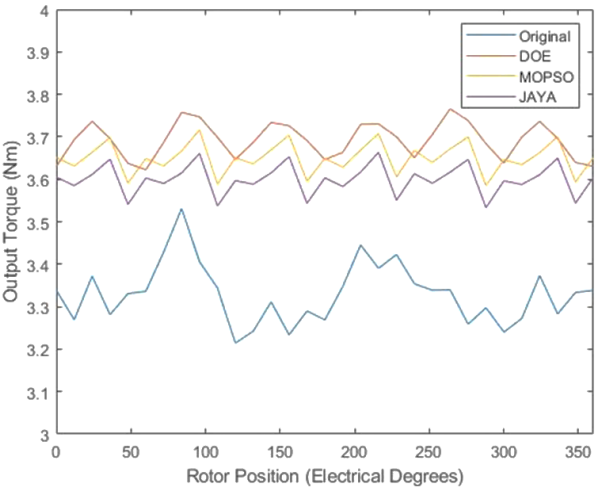

Fig. 6 Comparison of shaft output torque in terms of torque ripple.

Similarly, the von Mises stress is observed to be 1 MPa in JAYA optimized model, which is also substantially smaller than the yield strength, ensuring a safe and reliable rotor design. The maximum distortion of the rotor was found to be significantly low 0.00006 mm as shown in Fig. 8 for JAYA optimized model.

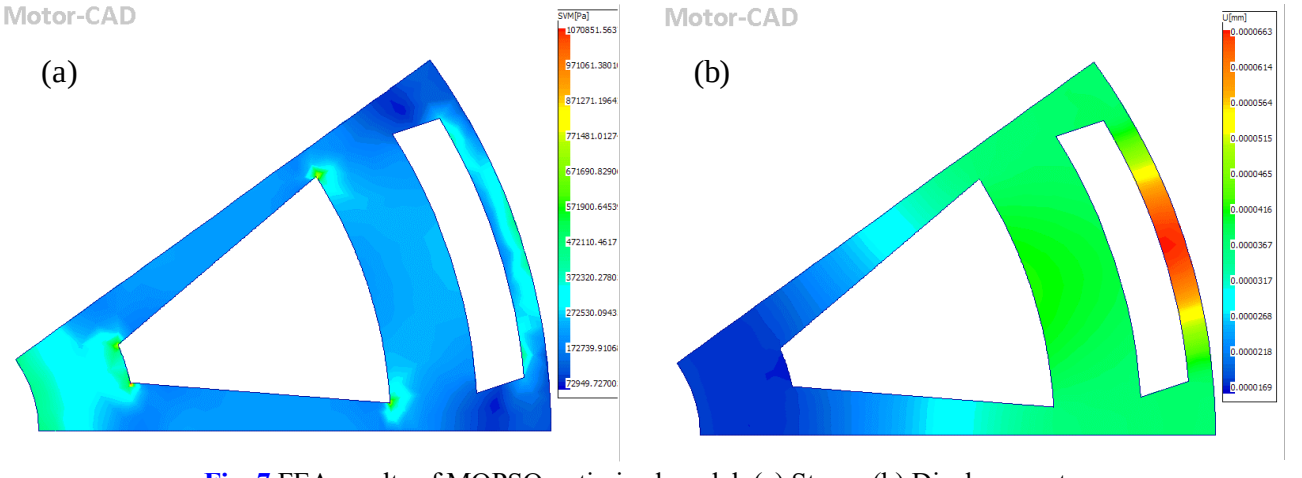

Fig. 7 FEA results of MOPSO optimized model. (a) Stress, (b) Displacement.

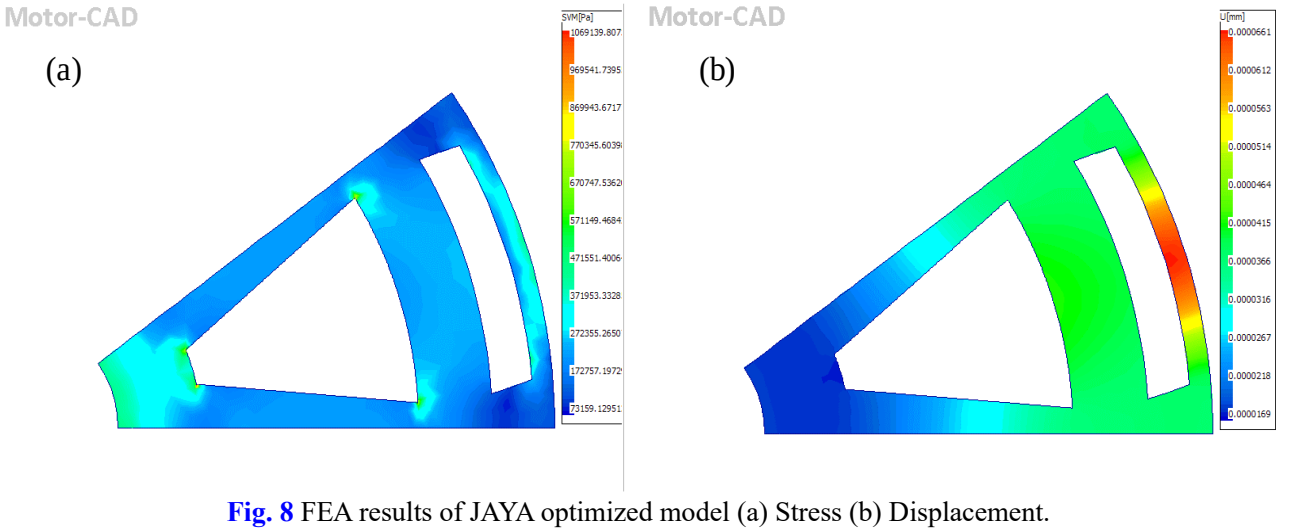

Fig. 8 FEA results of JAYA optimized model (a) Stress (b) Displacement.

5. Conclusions

In this work, torque ripples and cogging torque in IPMSM were significantly reduced utilizing PSO, JAYA, ANN, and the orthogonal experimental approach. Initially, in the orthogonal experiment technique, motor geometric parameters were employed as factors, while torque ripples, cogging torque, and shaft output torque were utilized as responses. Later the regression equations were obtained for the responses using MINITAB software and the ANN model. The ANN provided a better fit. Finally, the ANN model has been employed in the multi-objective optimization PSO and JAYA algorithms. Torque ripples and cogging torque were reduced by 65% and 12%, respectively, after optimization. The shaft output torque was increased by 9%. The optimization outcomes demonstrated that the methods used in this study were capable of obtaining optimal design variables with reduced IPMSM torque ripple and cogging torque. The results show that the design goal of finding optimal variables can be successfully satisfied using the proposed hybrid method of optimization using ANN in conjunction with the design of experiments.

Acknowledgments

The authors acknowledge the support provided by the Manipal Institute of Technology, Manipal Academy of Higher Education, Manipal, for carrying out the research work.

Conflict of Interest

The authors declare no conflict of interest.

Supporting information

Applicable.

References

[1] M. Li, W. Wang, *Micromotors*, 2018, **51**, 11–14.
[2] Q. Liu, K. Hameyer, *IEEE Transactions on Industry Applications*, 2016, **52**, 4855–4864, doi: 10.1109/TIA.2016.2599902.
[3] F. L. Langley, P. Mellor, *3rd IET international conference on power electronics, machines and drives,* 2006, 489-493.
[4] L. Parsa, L. Hao, *IEEE Transactions on Industry Applications*, 2008, **55**, 602-609, doi: 10.1109/TIE.2007.911953.
[5] X. Zhu, W. Wu, L. Quan, Z. Xiang, W. Gu, *IEEE Transactions on Energy Conversion*, 2019, **34**, 1178-1189, doi: 10.1109/tec.2018.2886316.
[6] A. Kioumarsi, M. Moallem, B. Fahimi, *IEEE Transactions on Magnetics*, 2006, **42**, 3706-3711, doi: 10.1109/tmag.2006.881093.
[7] Q. Zhu, S. Ruangsinchaiwanich, N. Schofield, D. Howe, *IEEE Transactions on Magnetics*, 2003, **39**, 3238-3240, doi: 10.1109/tmag.2003.816733.
[8] M. H. Hwang, J. H. Han, D. H. Kim, H. R. Cha, *Energies*, 2018, **11**, 2601, doi: 10.3390/en11102601.
[9] F. Ma, H. Yin, L. Wei, G. Tian, H. Gao, *Sustainability*, 2018, **10**, 1533, doi: 10.3390/su10051533.
[10] G. Zhang, W. Yu, W. Hua, R. Cao, H. Qiu, A. Guo, *Applied Sciences*, 2019, **9**, 3634, doi: 10.3390/app9173634.
[11] S. Zhu, W. Chen, M. Xie, C. Liu, K. Wang, *IEEE Transactions on Magnetics*, 2018, **54**, 1-5, doi: 10.1109/tmag.2018.2841851.
[12] M. H. Hwang, H. S. Lee, H. R. Cha, *Energies*, 2018, **11**, 3053, doi: 10.3390/en11113053.
[13] C. Hwang, C Chang, P. Li, C. Liu, *Journal of Physics: Conference Series*, 2011, **266**, 12068, doi: 10.1088/1742-6596/266/1/012068.
[14] K. I. Laskaris, A. G. Kladas, *IEEE Transactions on Industrial Electronics*, 2010, **57**, 138-145, doi: 10.1109/TIE.2009.2033086.
[15] J. Zheng, W. Zhao, C. H. T. Lee, J. Ji, G. Xu, *CES Transactions on Electrical Machines and Systems*, 2019, **3**, 12-18, doi: 10.30941/cestems.2019.00003.
[16] G. Lei, J. Zhu, Y. Guo, C. Liu, B. Ma, *Energies*, 2017, **10**, 1962, doi: 10.3390/en10121962.
[17] K. Abbaszadeh, F. Rezaee Alam, S. A. Saied, *Energy Conversion and Management*, 2011, **52**, 3075-3082, doi: 10.1016/j.enconman.2011.04.009.
[18] T. Song, Z. Zhang, H. Liu, W. Hu, *IET Electric Power Applications*, 2019, **13**, 1157-1166, doi: 10.1049/iet-epa.2019.0069.
[19] S. Shimokawa, H. Oshima, K. Shimizu, Y. Uehara, J. Fujisaki, A. Furuya, H. Igarashi, *IEEE Transactions on Magnetics*, 2018, **54**, 1-4, doi: 10.1109/tmag.2018.2841364.
[20] H. Sasaki, H. Igarashi, *International Journal of Applied Electromagnetics and Mechanics*, 2019, **59**, 87-96, doi: 10.3233/JAE-171164.
[21] D. Sim, D. Cho, J. Chun, H. Jung, T. Chung, *IEEE Transactions on Magnetics*, 1997, **33**, 1880-1883, doi: 10.1109/20.582651.
[22] M. Ikeda, T. Hiyama, *IEE Proceedings - Electric Power Applications*, 2005, **152**, 1595, doi: 10.1049/ip-epa: 20050173.
[23] D. Bae, D. Kim, H. Jung, S. Hahn, C. Koh, *IEEE Transactions on Magnetics*, 1997, **33**, 1924-1927, doi: 10.1109/20.582668.
[24] J. Hao, S. Suo, Y. Yang, Y. Wang, W. Wang, X. Chen, *IEEE Access*, 2020, **8**, 27202-27209, doi: 10.1109/access.2020.2971473.
[25] Y. Zhang, S. Wang, G. Ji, *Mathematical problems in engineering*, 2015, **931256**, 1-38, doi: 10.1155/2015/931256.
[26] M. A. Abido, *Electric Power Systems Research*, 2009, **79**, 1105-1113, doi: 10.1016/j.epsr.2009.02.005.
[27] R. Venkata Rao, *International Journal of Industrial Engineering Computations*, 2016, **7**, 19–34, doi: 10.5267/j.ijiec.2015.8.004.
[28] R. A. Zitar, M. A. Al-Betar, M. A. Awadallah, I. A. Doush, K. Assaleh, *Archives of Computational Methods in Engineering*, 2021, 1-30, doi: 10.1007/s11831-021-09585-8.

Author Information

Mr. Ganesh C. J. *is pursuing his Master of Technology in Computer Aided Analysis and Design at Manipal Institute of Technology, MAHE, Manipal. His current interests include Design of Experiments, Optimization methods and Product design & analysis.*

Dr. Vijay G. S. *is Professor in the Department of Mechanical and Industrial Engineering at Manipal Institute of Technology, MAHE, Manipal, India. Bearing Diagnostics; Application of Soft Computing Techniques to Engineering and non-Engineering domains; Machinery Vibration Signal Processing and Analysis; Finite Element Analysis; Geometric Modelling for CAD; Mechanical Vibrations; Fluid Mechanics; Operations Research; Material Science and Metallurgy are the areas of his expertise.*

Dr. Siddappa Bekinal *is an Associate Professor in the Department of Mechanical and Industrial Engineering at Manipal Institute of Technology, MAHE, Manipal, India. Passive Magnetic Bearings; Mechanical Vibrations; Rotor Dynamics; Turbomachinery and Mechanical Vibrations Energy Harvesting are the areas of his expertise.*